J Supercond Nov Magn (2013) 26:2603–2606
DOI 10.1007/s10948-013-2143-2

ORIGINAL PAPER

Distribution of Optical Spectral Weight in Detwinned $Ba(Fe_{1-x}Co_x)_2As_2$

A. Dusza · A. Lucarelli · J.-H. Chu · I.R. Fisher · L. Degiorgi

Received: 2 December 2012 / Accepted: 14 February 2013 / Published online: 22 March 2013

Abstract We analyze our recent optical investigation on detwinned $Ba(Fe_{1-x}Co_x)_2As_2$ materials in the underdoped regime from the perspective of the spectral weight (*SW*) distribution. We identify its evolution for both in-plane crystallographic axes as a function of temperature across the structural tetragonal-orthorhombic phase transition. We can thus disentangle the anisotropy of *SW* occurring in the orthorhombic magnetic phase, from where we identify the relevant energy scales arising from interactions with spin fluctuations.

Keywords Iron-pnictide superconductors · Optical properties

Several quantum states are intimately connected with electronic correlations, mainly mediated by the strength of the repulsive interactions among electrons. Particularly in the context of superconductivity and more specifically with the discovery of the high temperature cuprate and iron-pnictide superconducting materials [1, 2], the role played by correlations is of stringent importance and is still matter of intense investigations.

A. Dusza · A. Lucarelli · L. Degiorgi (✉)
Laboratorium für Festkörperphysik, ETH–Zürich, 8093 Zürich, Switzerland
e-mail: degiorgi@solid.phys.ethz.ch

J.-H. Chu · I.R. Fisher
Geballe Laboratory for Advanced Materials and Department of Applied Physics, Stanford University, Stanford, CA 94305-4045, USA

J.-H. Chu · I.R. Fisher
Stanford Institute for Materials and Energy Sciences, SLAC National Accelerator Laboratory, 2575 Sand Hill Road, Menlo Park, CA 94025, USA

In the cuprates electronic correlations are so strong that the parent compounds, out of which superconductivity originates, are Mott insulator. On the other hand, there is mounting evidence that the parent compounds of the iron-pnictide superconductors are bad metals, where electronic correlations are sufficiently strong to place them close to the boundary between itinerancy and interaction-induced electronic localizations [3]. Moreover in both families, superconductivity develops when magnetism, characterizing in part their phase diagram, is destroyed by dopings. This led to the conjecture that exchange of magnetic fluctuations may provide the glue, binding electrons into Cooper pairs [4].

The effects of electronic correlations lead to significant fingerprints in several measurable physical quantities. A direct impact of correlations may be recognized in the charge dynamics; namely, through the distribution of spectral weight (*SW*), encountered in the real part $\sigma_1(\omega)$ of the optical conductivity. *SW* is generically defined as integral of $\sigma_1(\omega)$ ($SW = \int_0^{\omega_c} \sigma_1(\omega)\, d\omega$) up to the cut-off frequency ω_c. The optical response can be achieved nowadays with great precision over an extremely broad spectral range, a prerequisite of paramount importance in order to perform reliable integration of $\sigma_1(\omega)$.

Since electronic correlations significantly impede the mobility of the electrons, they consequently lead to a substantial reduction of the Drude weight of the itinerant charge carriers with respect to the expectation for nearly free or non-interacting particles. Precisely, one has to distinguish among two cases; namely, quenching the Drude weight by local (Hubbard-like) correlations or by interactions with a bosonic mode (i.e., phonons or spin fluctuations) [4–7].

Qazilbash et al. recently made an interesting survey about the impact of the electronic correlations by looking to a wealth of materials, ranging from conventional metals to Mott insulators [8]. They proposed a quantitative approach

based on the calculation of the optical (K_{opt}) and band (K_{band}) kinetic energy. K_{opt} is obtained from the integral of the effective (Drude) metallic component of the optical conductivity (also referred to as the coherent part of the single electron excitations in an interacting metallic system), while K_{band} (also known as the kinetic energy of the underlying non-interacting system) is extracted from ab initio (tight-binding) band-structure calculations neglecting the electron-electron interactions [3]. The ratio K_{opt}/K_{band} may be considered as representative quantity displaying the degree of electronic correlations. K_{opt}/K_{band} close to one corresponds to the nearly free, non-interacting limit, while close to zero would imply a Mott-insulating state [3, 8].

Alternatively, a fully experimentally based spectral weight analysis of the excitation spectrum, free from any theoretical or band-structure assumptions, was proposed by Ref. [9]. The total spectral weight encountered in the optical conductivity up to the onset of the electronic interband transitions, which is considered to be representative of the expected weight in a normal (uncorrelated) metallic state, turns out to be usually redistributed into a well-distinct (narrow) Drude resonance and a so-called incoherent part, identified with a generic MIR-band of $\sigma_1(\omega)$. Thus, by discussing several materials a rather clear-cut evidence has been given that the reduction of the (Drude) metallic spectral weight in the excitation spectrum with respect to the total one, both evinced experimentally, may provide an opportunity to establish the strength of interaction (electron-electron as well as electron-phonon) [9].

In this communication, we wish to primarily focus our attention on spectral weight issues related to the iron-pnictides. First of all, we shall mention that, motivated by the work reported in Ref. [8], we undertook a systematic optical investigation of the Co-doped $BaFe_2As_2$ family [10], for several compositions spanning the entire phase diagram [11]. We argue that these 122 iron-pnictides fall in the regime of moderate electronic correlations for the parent compounds and close to optimal doping, while a conventional metallic behavior in the nearly free electron limit is recovered at the opposite, overdamped end of the superconducting dome [10]. The main bulk of our claims was then lately confirmed by Schafgans et al. [12], who further proposed that Hund's coupling is the primary mechanism giving rise to correlations.

However, it is well known that the 122 systems tend to naturally twin when crossing the structural tetragonal-orthorhombic phase transition in the underdoped regime. This means that so far we just achieved the averaged view of the spectral weight evolution, since with optical probes we addressed several, randomly oriented domains. Large magnetic field and applied uniaxial pressure have been shown to be very effective as well as quite efficient ways in order to totally detwinned the specimens [13]. For samples held under uniaxial pressure, it was possible to disentangle the anisotropy of the orthorhombic phase in various measurable physical quantities. This led to a vigorous debate with respect to scenarios based on a purely electronic origin (e.g., via orbital ordering) or on a spin-induced nematic phase for the structural transition [13]. Therefore, we specifically turn here our attention to detwinned specimens, in order to enhance and better appreciate the anisotropic *SW* evolution with respect to the axes of the orthorhombic phase.

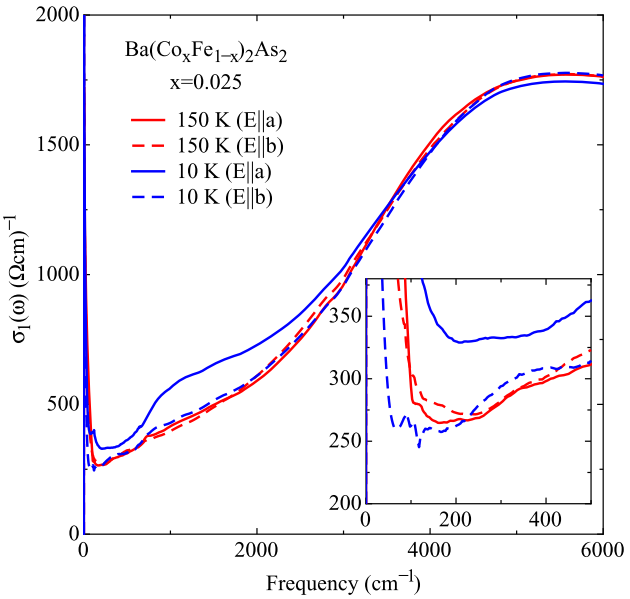

Fig. 1 Real part $\sigma_1(\omega)$ of the optical conductivity of $Ba(Co_xFe_{1-x})_2As_2$ for $x = 2.5$ % in the near- and mid-infrared spectral range at selected temperatures above and below the structural phase transition at T_s. The *inset* displays $\sigma_1(\omega)$ in the far-infrared, emphasizing the anisotropy of the effective metallic contribution to the excitation spectrum [16] (Color figure online)

Our experiment consists of measuring the optical reflectivity as a function of temperature over a broad spectral range, extending from the far-infrared up to the ultraviolet. This is the prerequisite in order to perform reliable Kramers–Kronig transformation leading to all optical functions, including $\sigma_1(\omega)$ [14]. We direct the readership to our Refs. [15, 16] for a comprehensive description of our experiment and the full display of the results.

In order to set the stage for the present discussion, we reproduce in Fig. 1 $\sigma_1(\omega)$ achieved on the 2.5 % Co-doped 122 material, held under uniaxial pressure. The structural transition for this composition occurs at $T_s \sim 98$ K, which precedes the magnetic one at $T_N \sim 92$ K [11]. There is an obvious anisotropy in the mid-infrared (MIR) range, as displayed in the main panel, when comparing $\sigma_1(\omega)$ along the orthorhombic a- and b-axis at low temperatures. Such an anisotropy extends down to low frequencies into the far-infrared (FIR), as shown in the inset of Fig. 1. The anisotropy progressively develops with decreasing tempera-

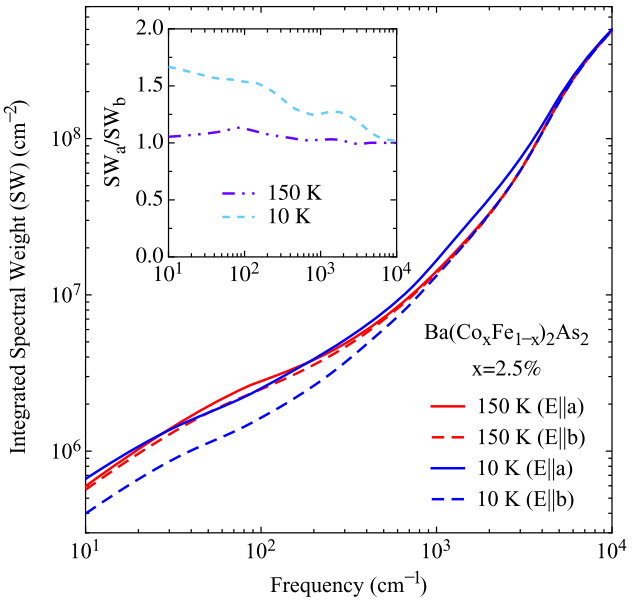

Fig. 2 Integrated spectral weight (*SW*) for both polarization directions at selected temperatures above and below the structural phase transition at T_s. The *inset* displays the ratio of *SW* between the two polarization directions (i.e., orthorhombic *a*- and *b*-axis) at 10 and 150 K (Color figure online)

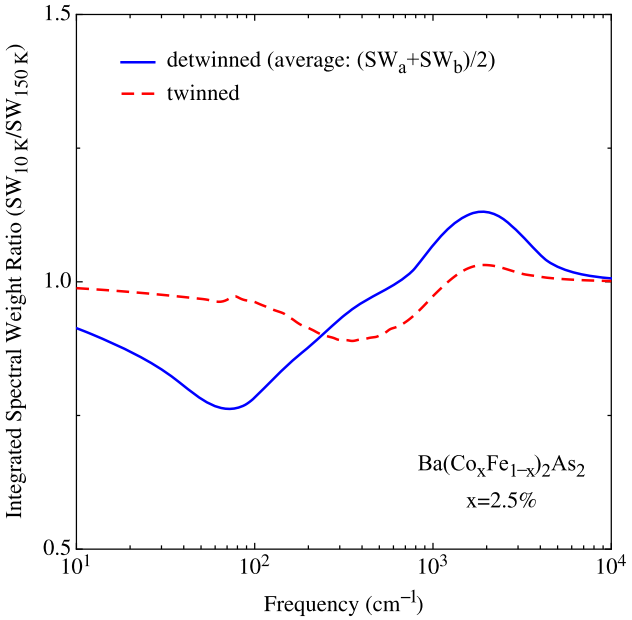

Fig. 3 Ratio of the averaged integrated spectral weight ($SW = (SW_a + SW_b)/2$) between 10 and 150 K for the detwinned sample, compared to the same ratio for data collected on the twinned specimen [16] (Color figure online)

ture already from above T_s and is then fully deployed when entering the orthorhombic phase (Fig. 1) [16]. This optical anisotropy is directly linked to the linear dichroism. We emphasized moreover that the temperature dependence of such a dichroism at all dopings scales with the anisotropy ratio of the *dc* conductivity [13, 17], suggesting the electronic nature of the structural transition. Our findings bear testimony to a large nematic susceptibility that couples very effectively to the uniaxial lattice strain [15, 16].

We can now integrate $\sigma_1(\omega)$ up to a cut-off frequency at each temperature and for both polarizations. Such an integrated *SW* is depicted in Fig. 2 as a function of the (cut-off) frequency, continuously varying from zero to 10^4 cm^{-1}, and for two representative temperatures above and below T_s. At 150 K, *SW* is almost fully isotropic, indicating the absence of polarization dependence between both axes (Fig. 1). When lowering the temperature below T_s with the sample held under uniaxial pressure, an obvious anisotropy in *SW* develops; along the *a*-axis there is a shift of spectral weight mainly in the range between 1000 and 3000 cm^{-1} (i.e., into the MIR feature peaked at about 1500 cm^{-1} in $\sigma_1(\omega)$, see Fig. 1) as well as into the FIR range, leading to an enhancement of the Drude component (inset of Fig. 1) [16], while along the *b*-axis there is a depletion of *SW*, which clearly manifests the opening of the pseudogap [10]. The removed *SW* along *b* mainly shifts at higher energies. In order to emphasize these trends, the inset of Fig. 2 displays the *SW* ratio between the *a*- and *b*-axis at the two selected temperatures above and below T_s. Far above T_s (i.e., at 150 K) the ratio is barely deviating from unity, thus implying an isotropic optical response. Within the orthorhombic magnetic state (i.e., at 10 K), the enhancement of *SW* along the *a*-axis with respect to the *b*-direction at FIR and MIR energy scales is obvious. Although not shown here, a similar *SW* evolution in temperature and with respect to both polarization directions has been observed for the parent ($x = 0$) and $x = 4.5$ % compound, as well. For $x = 0$ the pseudogap formation in the magnetic state along the *b*-axis is even more pronounced. Interestingly enough, the total *SW* for all Co-dopings is fully recovered at energy scales of about 10^4 cm^{-1} (Fig. 2), consistent with Ref. [12].

We have repeatedly emphasized the importance to perform measurements on detwinned, single domain specimens. For instance, investigation of the electronic structure and the mapping of the reconstructed Fermi surface via ARPES [18] clearly pointed out that their anisotropy in the magnetic orthorhombic phase is remarkably masked when addressing twinned specimens with respect to detwinned ones. Before going any further with our concluding remarks, we wish to similarly suggest a comparison between twinned and detwinned specimens in terms of our *SW* analysis. We may assume that the averaged $SW = (SW_a + SW_b)/2$, obtained from the investigation of detwinned materials along the *a*- and *b*-axis (Fig. 2), is an ideal representation of the total *SW* which we may expect when integrating directly the optical conductivity collected on twinned specimens [10]. Indeed, Fig. 3 displays such a comparison in terms of the *SW* ratio between 10 and 150 K. Keeping in mind that we

are dealing with data collected in different experiments and on different specimens and that within our assumption the contributions from the a- and b-axis of the orthorhombic phase are assumed to be equivalent, the proposed comparison is astonishingly good. The averaged view of the *SW* distribution points out the removal of weight in the infrared region, which piles up in the MIR feature and leads to the opening of a pseudogap-like absorption in $\sigma_1(\omega)$ [10]. The enhancement of weight, observed at FIR frequencies, denotes the formation of a narrow Drude response at low temperatures, which is the coherent part of the excitation spectrum. While the averaged *SW* analysis on twinned materials yet allows us to identify the relevant energy intervals (Fig. 3), it washed out the detailed view with respect to both orthorhombic axes.

Supporting our thorough optical investigation on detwinned 122 materials [15, 16] with the present *SW*-arguments leads us to propose that for temperatures below the Neel transition, the topology of the reconstructed Fermi surface, combined with the distinct behavior of the scattering rates (i.e., the width of the effective Drude component in $\sigma_1(\omega)$, inset of Fig. 1 [16]), determines the anisotropy of the low frequency optical response. For the itinerant charge carriers, we are thus able to distinguish the evolution of the Drude weights and scattering rates and to observe their enhancement and depletion or reduction along the orthorhombic antiferromagnetic a-axis and ferromagnetic b-axis, respectively. The anisotropy of the optical conductivity, discussed so far in the dc limit, extends to high frequencies in the mid- and near-infrared regions. The related reshuffling of *SW* (Fig. 2) gives rise to the MIR feature at about 1500 cm^{-1} in $\sigma_1(\omega)$ (Fig. 1). The latter was linked to the magnetic spin-stripe order, which was also shown to correspond to the energy-minimum configuration within LAPW calculations [16, 19].

In summary, we exploited our optical results, collected on the title, detwinned compounds in the underdoped regime from the perspective of the *SW* analysis. From this *SW* analysis, we clearly identify two relevant energy scales: at about 1500 cm^{-1}, representative for the SDW state, and at approximately 10^4 cm^{-1}, which denotes the recovery of *SW* in the paramagnetic state. The coherent metallic part mainly develops along the orthorhombic a-axis, while the SDW state leading to the depletion of *SW* and the opening of the pseudogap-like excitation affects principally the orthorhombic b-axis.

Acknowledgements The author wishes to thank M. Dressel, L. Benfatto, A. Millis, D. Basov, M. Qazilbash and A. Chubukov for fruitful discussions. This work has been supported by the Swiss National Foundation for the Scientific Research within the NCCR MaNEP pool.

References

1. Bednorz, J.G., et al.: Z. Phys. B **64**, 189 (1986)
2. Kamihara, Y., et al.: J. Am. Chem. Soc. **130**, 3296 (2008)
3. Si, Q.: Nat. Phys. **5**, 629 (2009)
4. Mazin, I.I.: Nature **464**, 183 (2010)
5. Benfatto, L.: private communication
6. Benfatto, L., et al.: Phys. Rev. B **80**, 214522 (2009)
7. Ortenzi, L., et al.: Phys. Rev. Lett. **103**, 046404 (2009)
8. Qazilbash, M.M., et al.: Nat. Phys. **5**, 647 (2009)
9. Degiorgi, L.: New J. Phys. **13**, 023011 (2011)
10. Lucarelli, A., et al.: New J. Phys. **12**, 073036 (2010)
11. Chu, J.-H., et al.: Phys. Rev. B **79**, 014506 (2009)
12. Schafgans, A.A., et al.: Phys. Rev. Lett. **108**, 147002 (2012)
13. Fisher, I.A., Degiorgi, L., Shen, Z.X.: Rep. Prog. Phys. **74**, 124506 (2011) and references therein
14. Dressel, M., Grüner, G.: Electrodynamics of Solids. Cambridge University Press, Cambridge (2002)
15. Dusza, A., et al.: Europhys. Lett. **93**, 37002 (2011)
16. Dusza, A., et al.: New J. Phys. **14**, 023020 (2012)
17. Chu, J.-H., et al.: Science **329**, 824 (2010)
18. Yi, M., et al.: Proc. Natl. Acad. Sci. USA **108**, 6878 (2011)
19. Sanna, A., et al.: Phys. Rev. B **83**, 054502 (2011)